

Coronal waves and oscillations

Valery M. Nakariakov

Physics Department, University of Warwick, Coventry CV4 7AL, United Kingdom
email: V.Nakariakov@warwick.ac.uk

Abstract. Wave and oscillatory activity of the solar corona is confidently observed with modern imaging and spectral instruments in the visible light, EUV, X-ray and radio bands, and interpreted in terms of magnetohydrodynamic (MHD) wave theory. The review reflects the current trends in the observational study of coronal waves and oscillations, theoretical modelling of interaction of MHD waves with plasma structures, and implementation of the theoretical results for the mode identification. Also the use of MHD waves for remote diagnostics of coronal plasma - MHD coronal seismology - is discussed.

Keywords. (magnetohydrodynamics:) MHD, waves, Sun: corona, Sun: flares, Sun: oscillations, Sun: magnetic fields

1. Introduction

Wave and oscillatory phenomena in the corona have been attracting researcher's attention for several decades. Traditionally, the interest to coronal waves and oscillations is motivated by the possible role the waves playing in heating of the corona and in acceleration of the solar wind, via the transfer and deposition of energy and mechanical momentum. Also, as waves and oscillations are associated with various dynamical processes in the almost fully ionised and highly magnetised coronal plasma, hence their study is fundamental for plasma astrophysics in general. Moreover, the progress recently reached in observational detection and theoretical modelling of coronal waves and oscillations provided us with the foundation for *coronal seismology* - a new and rapidly developing branch of astrophysics, which combines theoretical and observational findings in deducing information about physical parameters in the corona.

An important role in the interpretation of coronal wave and oscillatory phenomena is played by magnetohydrodynamic (MHD) theory. Indeed, the observed characteristic scales, e.g. wave lengths, are usually much larger than both the ion gyroradius and the mean free path length and the characteristic times are much greater than the ion gyroperiod and the reciprocal of the collision frequency. Compressibility and elasticity of the coronal plasma allow it to support various kinds of MHD waves which are associated with perturbations of macro parameters of the plasma: its mass density, temperature, gas pressure, bulk velocity, and the magnetic field. Detection of MHD perturbations in the coronal plasma as fluctuations of emission intensity of coronal lines, their Doppler shifts and non-thermal broadening, and radio emission, provides us with the basis for the observational study of MHD waves in the corona.

More detailed recent reviews of this topic can be found in Aschwanden (2004) and Nakariakov & Verwichte (2005).

2. MHD modes of a magnetic cylinder

A cornerstone of coronal wave theory is dispersion relations for modes of a magnetic cylinder. Magnetic cylinders are believed to model well such common coronal structures

as coronal loops, various filaments, polar plumes, etc. Consider a straight cylindrical magnetic flux tube of radius a filled with a uniform plasma of density ρ_0 and pressure p_0 within which is a magnetic field $B_0\mathbf{e}_z$; the tube is confined to $r < a$ by an external magnetic field $B_e\mathbf{e}_z$ embedded in a uniform plasma of density ρ_e and pressure p_e (here we neglect the effects of magnetic field twist and curvature, as well as equilibrium steady flows).

In the internal and external media, the sound speeds are C_{s0} and C_{se} , the Alfvén speeds are C_{A0} and C_{Ae} , and the tube speeds are C_{T0} and C_{Te} , respectively. Relations between those characteristic speeds determine properties of MHD modes guided by the tube.

The presence of a characteristic spatial scale, the radius of the tube a , brings wave dispersion. The standard derivation of linear dispersion relations is based upon linearisation of MHD equations around the equilibrium.

Matching external and internal solutions of linearised MHD equations at the cylinder boundary, one can derive the dispersion relation for magnetoacoustic waves in a magnetic flux tube (Zaitsev & Stepanov 1975; Roberts *et al.* 1984; see also Nakariakov & Verwichte 2005 for more detail),

$$\rho_e(\omega^2 - k_z^2 C_{Ae}^2)\kappa_0 \frac{I'_m(\kappa_0 a)}{I_m(\kappa_0 a)} + \rho_0(k_z^2 C_{A0}^2 - \omega^2)\kappa_e \frac{K'_m(\kappa_e a)}{K_m(\kappa_e a)} = 0. \tag{2.1}$$

Here κ_0 and κ_e play a role of transverse wave numbers and are defined as

$$\kappa_\alpha^2 = \frac{(k_z^2 C_{s\alpha}^2 - \omega^2)(k_z^2 C_{A\alpha}^2 - \omega^2)}{(C_{s\alpha}^2 + C_{A\alpha}^2)(k_z^2 C_{T\alpha}^2 - \omega^2)} \tag{2.2}$$

with $\alpha = 0, e$; $I_m(x)$ and $K_m(x)$ are modified Bessel functions of order m , and the prime denotes the derivative of a function $I_m(x)$ or $K_m(x)$ with respect to argument x . For modes that are confined to the tube (evanescent outside, for $r > a$), the condition $\kappa_e^2 > 0$ has to be fulfilled. The integer m determines the azimuthal modal structure: waves with $m = 0$ are called *sausage* modes, waves with $m = 1$ are *kink* modes, waves with higher m are sometimes referred to as *flute* or *ballooning* modes. The existence and properties of the modes are determined by the equilibrium physical quantities. In particular, a coronal loop or a filament can trap MHD waves if the external Alfvén speed is greater than internal. Figure 1 shows a dispersion plot typical for an active region loop.

Thus, the main modes of solar coronal loops are: (a) a sausage (or radial, or $m = 0$) mode, which is periodic widening and contraction of the loop, this mode is essentially compressible and perturbs the absolute value of the magnetic field in the loop; (b) a kink (or transverse, or $m = 1$) mode, which produces periodic displacements of the loop axis; this mode is weakly compressible; (c) a torsional (or twisting) modes which does not perturb the boundary of the loop and is incompressible; (d) a longitudinal (or acoustic, or slow magnetoacoustic) mode, which consists of field-aligned flows and perturbations of the density; this mode does not produce significant perturbations of the boundary and is essentially compressible. The modes with higher azimuthal numbers m (ballooning or flute modes) are compressible and do perturb the loop boundary.

In the following, we consider the observational manifestation of these modes in the corona of the Sun.

3. Transverse (kink) oscillations of coronal loops

Since its discovery with the imaging telescope on board the Transition Region and Coronal Explorer (TRACE) (Aschwanden *et al.* 1999, Nakariakov *et al.* 1999), transverse

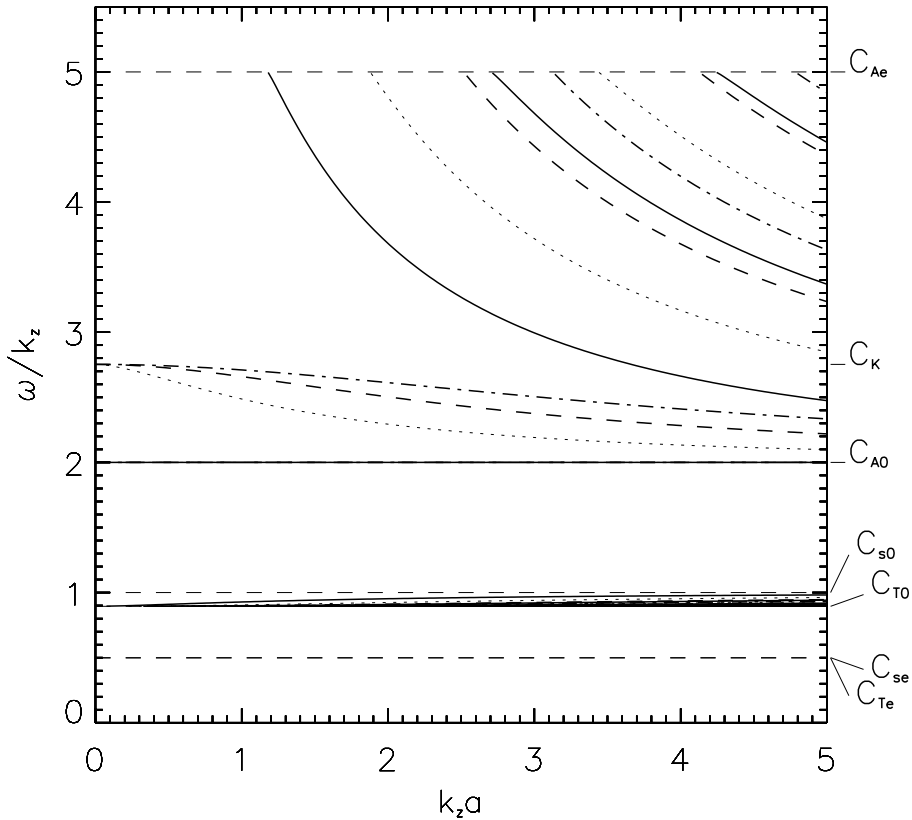


Figure 1. Dispersion diagram showing the phase speed solutions of dispersion relation (2.1) for MHD waves in a magnetic cylinder as a function of the dimensionless parameter $k_z a$. The typical speeds in the internal and external media are shown relative to the internal sound speed: $C_{A0} = 2 C_{s0}$, $C_{Ae} = 5 C_{s0}$ and $C_{se} = 0.5 C_{s0}$. The solid, dotted, dashed and dot-dashed curves correspond to solutions with the azimuthal wave number m equal to 0, 1, 2 and 3 respectively. The torsional Alfvén wave mode solution is shown as a solid line at $\omega/k_z = C_{A0}$. (From Nakariakov & Verwichte 2005)

oscillations of coronal loops are subject to an extensive observational and theoretical study. The oscillations are observed in both 171 Å and 195 Å lines as spatially resolved decaying periodic displacements of coronal loops, both on the solar disc and off-limb. The typical values of the periods are in the range from a few to several minutes and are different for different loops. The oscillations are observed to decay very quickly, just in a few wave periods. The displacement amplitude reaches several Mm, which exceeds the diameter of the oscillating loop. When the LOS has a significant component parallel to the plane of the oscillations, the kink mode can be detected with spectral instruments through the periodically modulated Doppler shift. Possibly, kink modes were found by Koutchmy *et al.* (1983) in the Doppler shift of the green coronal line. Best-fitting the displacement of a segment of the oscillating loop along a chosen slit perpendicular to the loop with a decaying harmonic function of the form

$$x(t) = A_0 \exp(t/t_d) \cos(2\pi t/P + \phi_0) \quad (3.1)$$

allows us to determine the oscillation period P and decay time t_d , along with the amplitude A and the initial phase ϕ_0 of the oscillation. Ofman & Aschwanden (2002) analysed eleven oscillating loops and determined a scaling law which connects the decay time and the period of transverse oscillations, $t_d \propto (a^2 P^2)^{0.33 \pm 0.08}$. However, oscillations in a post-flaring arcade, studied by Verwichte *et al.* (2004) were found to be inconsistent with this law. Results of the study of non-exponential decay laws, e.g., in the form of the function $\exp(t^N/t_d^N)$, where N is a constant (Verwichte *et al.* 2004, Nakariakov & Verwichte 2005), are not conclusive. It is still unclear which physical mechanism is responsible for the decay of kink oscillations.

In the majority of the observed events, only the global (or fundamental, or principle) mode of the oscillating loop was observed, with the wavelength equal to double the loop length. However, there can be higher spatial harmonics observed (Schrijver *et al.* 2002). In particular, the second harmonics was discovered by Verwichte *et al.* (2004) in an oscillating off-limb arcade.

The oscillation period of a global kink mode, with the wavelength much larger than the minor radius of the loop, is determined by the expression

$$P_{\text{GKM}} \approx \frac{2L}{C_K}, \tag{3.2}$$

where

$$C_{\text{GKM}} = \left(\frac{B_0^2/\mu_0 + B_e^2/\mu_0}{\rho_0 + \rho_e} \right)^{1/2} = \left(\frac{\rho_0 C_{A0}^2 + \rho_e C_{Ae}^2}{\rho_0 + \rho_e} \right)^{1/2}, \tag{3.3}$$

is a so-called *kink* speed, which corresponds to the density weighed average Alfvén speed, and L is the loop length. Using expression (3.3), Nakariakov & Ofman (2001) developed a method for the estimation of the absolute value of the magnetic field in an oscillating loop. For an analysed loop, this value was estimated as 13 ± 9 G. Verwichte *et al.* (2004) applied this method for the estimation of the magnetic field in an off-limb arcade. In these estimations, the main source of the error is the uncertainty in the measurement of the density, which is expected to be improved with the new generation of solar space missions.

4. Sausage oscillations

Sausage modes of coronal loops (as well as the kink modes) can be considered as modified fast magnetoacoustic waves, guided by the non-uniformity of the fast speed $C_F = \sqrt{C_A^2 + C_s^2}$. In the long wavelength limit, the phase speed of the sausage mode grows until it reaches the value of the Alfvén speed in the external medium. The cut-off wave number is

$$k_{zc} a = j_0 \left[\frac{(C_{s0}^2 + C_{A0}^2)(C_{Ae}^2 - C_{T0}^2)}{(C_{Ae}^2 - C_{A0}^2)(C_{Ae}^2 - C_{s0}^2)} \right]^{1/2}, \tag{4.1}$$

where $j_0 \approx 2.40$ is the first zero of the Bessel function $J_0(x)$. For longer wavelengths the mode is leaky and radiates its energy to the external medium. The period of a global sausage mode of a solar coronal loop is determined by the loop length,

$$P_{\text{GSM}} \approx \frac{2L}{C_{\text{ph}}}, \tag{4.2}$$

where C_{ph} is approximately equal to the Alfvén speed in the external medium, C_{Ae} , (Nakariakov *et al.* 2003). Trapped global sausage modes can exist only in relatively short loops, with the length smaller than π/k_{zc} to satisfy the condition of the $k_z > k_{zc}$. As

$C_{A0} < C_{Ae}$, the period of the global sausage mode is always shorter than the period of the global kink mode in the same loop.

First identification of a spatially resolved global sausage mode was made in the microwave band, with the Nobeyama Radioheliograph (Nakariakov *et al.* 2003, see also Melnikov *et al.* 2005 for a detailed study of this event observed with high spatial resolution in cm, mm and HXR bands). As the flaring loop observed was well resolved with NoRH, it made possible to study the properties of the microwave pulsations at different parts of the loop. Well pronounced quasi-periodic pulsations of the emission intensity with the period about 14–17 s were present at the top and in both legs of the loop and were found to be synchronous. In the loop of the observed length, $L = 25$ Mm, the global sausage mode with the period of 16 s should have the phase speed about 3,130 km/s. This value is consistent with the possible value for the Alfvén speed outside the loop, and hence the observed period is in a good agreement with the estimation given by Eq. (4.2).

5. Longitudinal (slow magnetoacoustic) oscillations

In the low- β coronal plasma, slow magnetoacoustic modes which propagate almost along the magnetic field are similar to usual acoustic waves. In the straight magnetic cylinder approximation, these waves are practically dispersionless and their phase speed is about the sound speed C_{s0} for all wave numbers. There can be a global longitudinal mode in a coronal loop, similar to the global kink and global sausage modes discussed above, with the period

$$P_{\text{long}} = 2L/C_{s0}. \quad (5.1)$$

The practical formula for the determination of the period is

$$P_{\text{long}}/s \approx 13 \times (L/\text{Mm})/\sqrt{(T/\text{MK})}. \quad (5.2)$$

The perturbations of the field-aligned plasma velocity and density in the global longitudinal mode are

$$V_s(s, t) \propto \cos\left(\frac{\pi C_s}{L}t\right) \cos\left(\frac{\pi}{L}s\right), \quad (5.3)$$

$$\rho(s, t) \propto \sin\left(\frac{\pi C_s}{L}t\right) \sin\left(\frac{\pi}{L}s\right), \quad (5.4)$$

where A is wave amplitude, L is loop length, and s is a distance along the loop with the zero at the loop top. Numerical simulations of the response of the plasma in a coronal loop to an impulsive energy deposition (Nakariakov *et al.* 2004) showed that a second longitudinal harmonics of these mode is excited more efficiently.

Recently, Doppler shift and intensity oscillations were discovered in coronal loops observed in the far UV Fe XIX and Fe XXI emission lines with SOHO/SUMER (Wang *et al.* 2002, 2003). This spectral line is associated with temperatures of about 6 MK, corresponding to the sound speed of about 370 km/s. The observed periods are in the range 7–31 min, with decay times 5.7–36.8 min, and show an initial large Doppler shift pulse with peak velocities up to 200 km/s. The intensity fluctuation, if observed, lags the Doppler shifts by 1/4 period. Ofman & Wang (2002) identified this mode as the longitudinal (or acoustic) mode. Unfortunately, the field-of-view of SUMER is a one-dimensional slit, making it impossible to determine whether the spatial structure of the observed oscillation along the loop is consistent with Eq. (5.3). However, the observed $\pi/4$ shift between velocity and density perturbations is also consistent with the theory. If the observational slit is positioned near the loop apex where the density perturbation has a

node (according to Eq. (5.3)), the observed Doppler shift is not accompanied by the line intensity variation, as is observed in the majority of cases. Concerning the decay of the oscillations, it was found that because of the high temperature of the loops, the large thermal conduction which depends on temperature as $T^{2.5}$, leads to rapid damping of the slow waves on a timescale comparable to observations.

This phenomenon can be quite wide-spread in flaring loop dynamics. Perturbations of the plasma density in this mode can produce the modulation of the intensity of thermal (e.g. soft X-ray, see the observational findings of McKenzie & Mullan, 1997) emission. Also, the density perturbations were recently found to be able to modulate efficiently gyrosynchrotron emission generated by non-thermal electrons in solar and stellar coronal flares (Nakariakov & Melnikov 2006). The modulation mechanism is based upon perturbation of the efficiency in Razin suppression of optically thin gyrosynchrotron emission. Modulation of the emission is in anti-phase with the density perturbation in the longitudinal wave. The observed emission modulation depth can be up to an order of magnitude higher than the slow wave amplitude. This effect is more pronounced in the lower part of the microwave spectrum.

As the period of longitudinal modes is determined by the sound speed which in its turn depends upon the temperature, the period should evolve with the loop temperature. Detection of such evolution would be a final proof of the existence of longitudinal standing modes in coronal loops.

There also are shorter wavelength propagating longitudinal waves observed in coronal loops and also in polar plumes.

6. Torsional modes

Torsional modes are incompressible and hence cannot be observed with coronal imagers. However, these modes can be detected through the variation of the non-thermal broadening with spectral instruments. Zaqarashvili (2003) suggested that the global torsional oscillations may be observed as a periodical variation of the spectral line width along the loop. The amplitude of the broadening is maximum at the velocity antinodes and minimum at the nodes of the torsional oscillation. Also, in the case of flaring loops, this mode can modulate microwave emission by the change of the angle between the LOS and the local magnetic field. The resonant period of an n -th standing torsional mode is

$$P_{\text{TM}} = 2L/nC_{A0}. \quad (6.1)$$

Observational evidence of the global torsional modes of coronal loops was found by Zaqarashvili (2003) and, possibly, by Grechnev *et al.* (2003).

7. Propagating fast wave trains

In a dispersive medium, impulsively generated (e.g., by an explosive energy release, such as a flare) waves evolve into a quasi-periodic wave train with pronounced period modulation. This effect is connected with dispersion of the initially broadband signal, as its different spectral components propagate at different phase and group speeds. In the coronal context, it was pointed out by Roberts *et al.* (1983, 1984) that periodicity of fast magnetoacoustic modes in coronal loops is not necessarily connected either with the wave source or with some resonances, but can also be created by the dispersive evolution of an impulsively generated signal. The dispersion is associated with the presence of a characteristic spatial scale, the minor radius of the loop which guides the fast waves.

Hence, the dispersion is more pronounced in the wavelengths comparable with the loop width. An estimation of the generated period is

$$P_{\text{prop}} = \frac{2\pi a}{j_0 C_{A0}} \sqrt{1 - \frac{\rho_e}{\rho_0}}, \quad (7.1)$$

where j_0 is the first root of the Bessel function. In loops with the large contrast ratio $\rho_e \ll \rho_0$, Eq. (7.1) reduces to $P_{\text{prop}} \approx 2.6a/C_{A0}$. We would like to stress that this period should be much shorter than the resonant periods of global modes, otherwise the wave train does not have sufficient distance to get developed. Consequently, this mechanism can operate in sufficiently long and thin loops only.

Numerical simulations of the developed stage of the dispersive evolution of a fast wave train in a smooth straight slab of a low but finite plasma- β plasma (Nakariakov *et al.* 2004) confirmed that development of an impulsively generated pulse leads to formation of a quasi-periodic wave train with the mean wavelength comparable with the slab width. In agreement with the analytical theory, the wave train has a pronounced period modulation which is best detected with the wavelet transform technique. In particular, it is found that the dispersive evolution of fast wave trains leads to the appearance of characteristic “tadpole” wavelet signatures (or, rather a “crazy tadpole” as it comes tail-first).

Rapidly propagating short-period compressible disturbances have recently been discovered with the SECIS coronal imaging instrument during a full solar eclipse (Williams *et al.* 2001, 2002) Propagating disturbances of the “green line” emission were observed to have a quasi-periodic wave train pattern with a mean period of about 6 s. As the observed speed was estimated at about 2,100 km/s, the disturbances were interpreted as fast magnetoacoustic modes. The comparison of the observed evolution of the wave amplitude along the loop with the theoretical prediction (Cooper *et al.* 2003) demonstrated an encouraging agreement. Katsiyannis *et al.* (2003) and Nakariakov *et al.* (2004) showed that wavelet spectra of the observed fast wave trains had the “crazy tadpole” wavelet signatures.

The effect of the dispersive formation of the wave train signature opens up interesting perspectives for MHD coronal seismology. The measurable properties of the wavelet tadpoles are the rates of the frequency and amplitude modulation, determined by the initial spectrum of the wave train, the distance of the region of observation from the wave source and by the loop profile. Multi-point observations can be used to exclude the first two parameters, providing us with the information about the loop profile, its steepness, possible sub-resolution structuring and filling factors.

Recently, Verwichte *et al.* (2005) presented for the first time a direct observational evidence of propagating fast waves in an open magnetic structure, a hot supra-arcade above a post-flare loop, observed with TRACE in 195Å. The supra-arcade is an open magnetic structure containing plume-like rays. In the particular event analysed, dark, tadpole-like structures appeared in the lanes between the rays. They were density depletions that moved sunwards, decelerating from speeds above 500 km/s to less than 100 km/s. The wave periods lie in the range of 90–220 s. The equivalent wavelengths are of the order of 20–40 Mm. Verwichte *et al.* interpreted these features as surface modes, which have the phase speed comparable with the Alfvén speed. If we assume that this speed lies plausibly in the range of 1,000–1,500 km/s, then there is quite a difference with the observed phase speeds, especially at lower heights. This discrepancy may be explained by the presence of fast upflows in the observed dark structures.

8. Conclusions

For recent several years, the study of wave and oscillatory phenomena has become one of the key elements of solar coronal physics, in the context of remote diagnostics of coronal plasmas, as well as in connection with the problems of coronal heating and solar wind acceleration. Recent observational discoveries in the EUV and microwave bands provide us with the evidence of several different standing MHD modes of coronal loops, including global transverse and sausage modes. There is also convincing information about the existence of standing acoustic and torsional modes of the loops, and direct imaging observations of propagating longitudinal waves and of fast magnetoacoustic wave trains. Theoretical modelling, based upon the straight magnetic cylinder approximation provides us with the solid foundation for the interpretation of these phenomena in terms of MHD waves and for the development of the coronal plasma diagnostic techniques.

References

- Aschwanden, M. J. 2004, *Physics of the Solar Corona*, Springer Praxis Books, Berlin
- Aschwanden, M. J., Fletcher, L., Schrijver, C. J., Alexander, D. 1999, *ApJ*, 520, 880
- Cooper, F. C., Nakariakov, V. M. & Williams, D. R. 2003, *Astron. Astrophys.*, 409, 325
- Grechnev, V. V., White, S. M. & Kundu, M. R. 2003, *ApJ*, 588, 1163
- Katsiyannis, A. C., *et al.* 2003, *Astron. Astrophys.*, 406, 709
- Koutchmy, S., Žugžda, I. D. & Locāns, V. 1983, *Astron. Astrophys.*, 120, 185
- McKenzie, D. E. & Mullan, D. J. 1997, *Solar Phys.*, 176, 127
- Melnikov, V. F., Reznikova, V. E., Shibasaki, K., Nakariakov, V. M. 2005, *Astron. Astrophys.*, 439, 727
- Nakariakov V. M., Arber T. D., Ault, C. E., Katsiyannis, A. C., Williams, D. R., Keenan, P. 2004, *MNRAS*, 349, 705
- Nakariakov, V. M., Melnikov, V. F. & Reznikova, V. E. 2003, *Astron. Astrophys.*, 412, L7
- Nakariakov, V. M. & Melnikov, V. F. 2006, *Astron. Astrophys.* 446, 1151
- Nakariakov, V. M. & Ofman, L. 2001 *Astron. Astrophys.* 372, L53
- Nakariakov, V. M., Ofman, L., DeLuca, E. E., Roberts, B., Davila, J. M. 1999, *Science*, 285, 862
- Nakariakov V. M., Tsiklauri D., Kelly A., Arber T. D., Aschwanden M. J. 2004, *Astron. Astrophys.* 414, L25
- Nakariakov, V. M., & Verwichte, E. 2005, *Living Rev. Solar Phys.*, 2, 3. URL(05/07/2005): <http://www.livingreviews.org/lrsp-2005-3>
- Ofman, L., & Aschwanden, M. J. 2002, *ApJ*, 576, L153
- Ofman, L. & Wang, T. 2002, *ApJ*, 580, L85
- Roberts, B., Edwin, P. M. & Benz, A. O. 1983, *Nature* 305, 688
- Roberts, B., Edwin, P. M. & Benz, A. O. 1984, *ApJ*, 279, 857
- Schrijver, C. J., Aschwanden, M. J. & Title, A. M. 2002, *Solar Phys.*, 206, 69
- Verwichte, E., Nakariakov, V. M. & Cooper, F. C. 2005, *Astron. Astrophys.* 430, L65
- Verwichte, E., Nakariakov, V. M., Ofman L., DeLuca E. E. 2004, *Solar Phys.* 223, 77
- Wang, T. J., Solanki, S. K., Curdt, W., Innes, D. E., Dammasch, I. E. 2002, *ApJ* 574, L101
- Wang, T. J., Solanki, S. K., Curdt, W., Innes, D. E., Dammasch, I. E., Kliem, B., 2003, *Astron. Astrophys.* 406, 1105
- Williams, D. R., *et al.* 2001, *MNRAS*, 326, 428
- Williams, D. R., *et al.* 2002, *MNRAS*, 336, 747
- Zaitsev, V. V. & Stepanov, A. V., 1975, *Issled. Geomagn. Aeron. Fiz. Solntsa*, 37, 3
- Zaqarashvili, T. V. 2003, *Astron. Astrophys.* 399, L15